npj | clean water

www.nature.com/npjcleanwater

ARTICLE OPEN

Check for updates

Highly durable and sustainable heterogeneous fabric using in-and-out fluorinated urethane coating for elimination of bacteria and oil–water separation

Moonhyun Choi[1], Sohyeon Park[1], Woojin Choi[1], Youna Kim[1], Kyeong Min Cho[2], Jiwoong Heo[1], Min-Kun Kim[2], Heesoo Jung[2], Youngho Jin[2]✉, Sangmin Lee[3]✉ and Jinkee Hong[1]✉

To address the poor oil–water separation efficiency and bactericidal properties of existing oil–water separation membranes for the treatment of industrial oily wastewater discharge, this study designed an in-and-out coating material for modifying the inner site and outer surface of porous activated carbon fabric (ACF) using urethane reactions. To this end, fluorinated polyurethane (F-PU) coating materials were synthesized using perfluoroalkyl alcohol, ethylene glycol (EG), and isophorone diisocyanate (IPDI). Subsequently, the inner and outer surface of the ACF were coated with F-PU via the urethane reaction of the hydroxyl groups (–OH) of the surface of ACF and the isocyanates of F-PU. The successfully fabricated in-and-out F-PU-coated heterogeneous fabric exhibited excellent hydrophobic properties, anti-scratch performance, oil–water separation performance, and bacterial penetration blocking efficiency (>99% for gram negative and gram positive bacteria). Furthermore, the in-and-out-coated ACF exhibited high durability, and retained its bacterial penetration blocking performance after scratch tests.

npj Clean Water (2022)5:48 ; https://doi.org/10.1038/s41545-022-00191-0

INTRODUCTION

The discharge of industrial oily wastewater and frequent oil spill accidents are causing increasingly severe water pollution problems, which have a catastrophic impact on the environment, particularly the aquatic ecological environment, and can result in huge economic loss[1–5]. For example, in July 2020, a Japanese bulk carrier broke off the Mauritius coast after spilling hundreds of tons of fuel oil. The spill included 814 metric tons of oil liquid waste, 318 metric tons of solid waste sludge, and contaminated debris. Accidents can occur at any time, and the cost of managing the after-effects of these accidents is enormous[6]. Therefore, it is essential to develop effective technologies for managing oil spills and harmful wastewater contaminants.

An increasing amount of oily wastewater is produced by several sources, and the efficient separation of these oil–water wastes has remained a significant challenge. Membrane filtration has attracted attention as an oil–water separation method owing to its convenience, low cost, environmental friendliness, and lack of requirement of chemicals or additives[7–10]. Accordingly, various studies have been conducted to functionalize the membrane filtration method to enhance its oil–water separation performance. For example, the use of superhydrophobic/superoleophobic coatings to control the wettability of membrane surface has been employed to enhance the various separation performance of this method[11–20].

However, in real-world environments, such as oil spills, there can be damages caused by external stimuli, as well as oil and water[21]. First, oily wastewater from industries contains different types of oil, lubricants and cooling agents, metal residues, and other organic and inorganic components[22,23]. In addition, oily wastewater from domestic sewage is composed of not only organic substances but also a significant number of pathogen microorganisms (e.g., bacteria, virus, and fungi). Second, oily wastewater sometimes contains solid lumps, which affect the flow of fluid through membrane surface; thus, damaging the membrane and reducing its performance[24]. Therefore, it is essential to develop innovative integrated removal processes based on filtration technologies owing to the varying characteristics and origin of the vast array of pollutants present in oily wastewater. Particularly, an ideal oil–water separation membrane should possess desirable surface wettability to achieve a high separation efficiency and permeability.

Versatile nanofiber fabrication electrospinning technique has been employed to fabricate nonwoven membranes containing continuous sub-micron or nano-sized entangled fibers[25–27]. Electrospun nanofibrous membranes have attracted attention for energy-saving and high-efficiency oil–water separation owing to their high porosity, high surface area-to-volume ratio, controllable pore size, and tunable morphology. However, the poor mechanical property of these membranes has limited their practical application. In addition, the poor long-term durability of current nanofibrous membranes in harsh environments has restricted its application. Therefore, it is essential to develop a novel functional membrane that can selectively and efficiently separate oil–water mixtures under harsh conditions.

Generally, anti-microbial materials and coatings are used in separation membranes to eliminate bacteria and drug release owing to their excellent bactericidal performance[28,29]; however, their side effects, such as the occurrence of super-bacteria, which can cause defects in the separation membrane, from continuous usage, have limited their further application[30]. In this study, we developed a highly durable porous fiber for oil–water separation and bacteria penetration blocking using an in-and-out fluorinated polyurethane (F-PU) coating. The F-PU materials was prepared via

[1]Department of Chemical & Biomolecular Engineering, College of Engineering, Yonsei University 50 Yonsei-ro, Seodaemun-gu, Seoul 03722, Republic of Korea. [2]Agency for Defense Development, Daejeon 34186, Republic of Korea. [3]School of Mechanical Engineering, Chung-ang University, Seoul 06974, Republic of Korea. ✉email: cadetnet@add.re.kr; slee98@cau.ac.kr; jkhong.yonsei@gmail.com

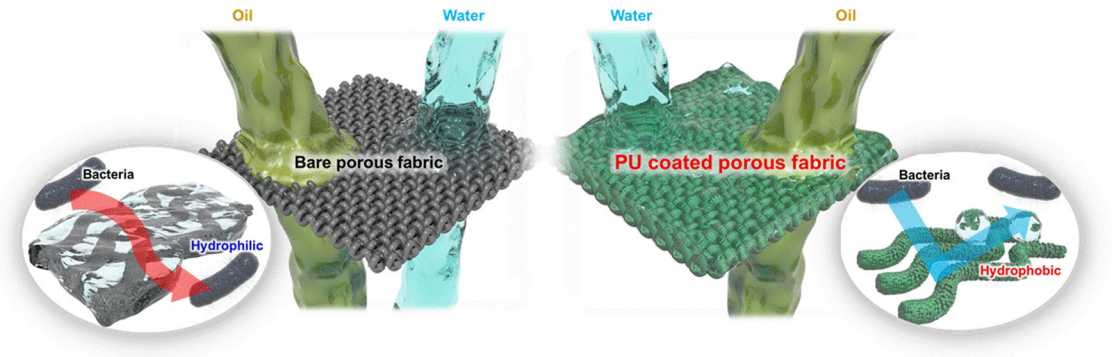

Fig. 1 Highly durable and sustainable heterogeneous fabric with in-and-out coatings. Schematic illustration of the in-and-out fluorinated polyurethane (F-PU)-coated fabric for oil–water separation and bacterial penetration blocking.

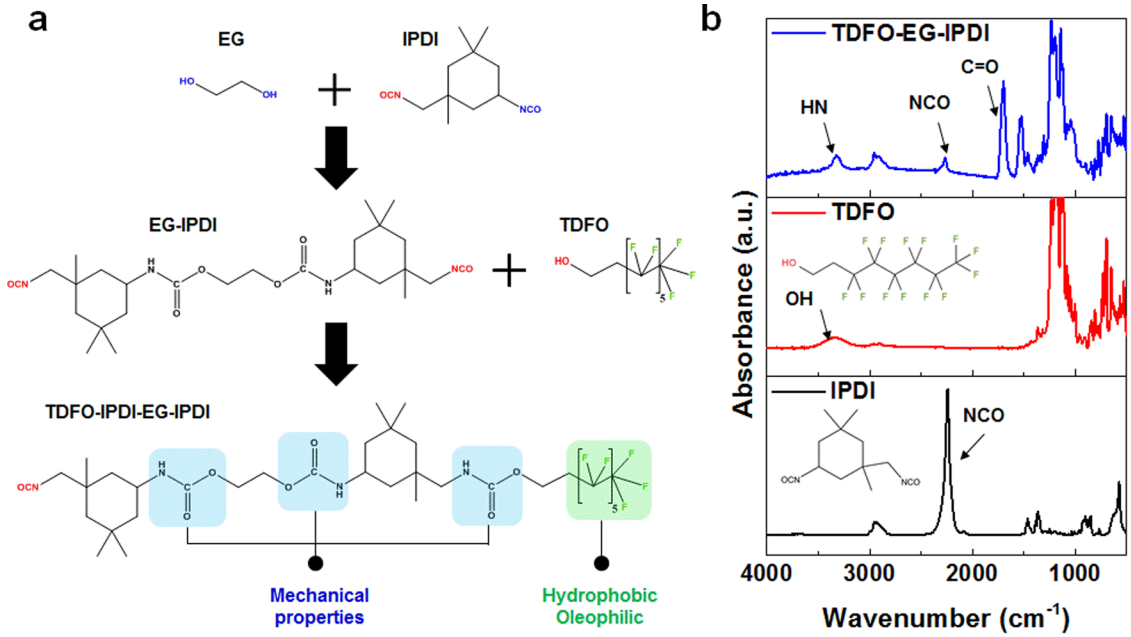

Fig. 2 Synthesis of in-and-out F-PU coating materials. a Schematic illustration of F-PU coating materials with the fluorination and urethane bonding of ethylene glycol (EG), isophorone diisocyanate (IPDI), and 1H,1H,2H,2H-Tridecafluoro-1-n-octanol (TDFO) for the synthesis of the F-PU coating materials (**b**) Fourier transform-infrared (FT-IR) transmittance of the F-PU coating materials (TDFO-IPDI-EG-IPDI), TDFO, and IPDI.

the urethane reaction of perfluoroalkyl alcohol, ethylene glycol (EG), and isophorone diisocyanate (IPDI). The prepared F-PU coating materials easily permeated and reacted in the inner site and outer surface of porous fibers. The in-and-out F-PU coating was used to fabricate a coated heterogeneous fabric, and the fabric exhibited excellent highly hydrophobic properties, anti-scratch performance, oil–water separation performance, and anti-bacterial effects (Fig. 1). Furthermore, the fabric maintained its bacterial penetration blocking ability even after the membrane was subjected to a scratching test; thereby, verifying the high durability of the fabricated in-and-out F-PU-coated fabric.

RESULTS AND DISCUSSION

In this study, in-and-out F-PU coating materials were synthesized using urethane reaction. The synthesis pathway of the F-PU coating materials is shown in Fig. 2a. The F-PU coating material was synthesized using IPDI, EG, and TDFO. One molecule of the F-PU coating material consisted of three urethane bonds, one NCO group, and one perfluoroalkyl group. The three urethane bonds reinforced the mechanical properties of the material by bonding hydrogen bonds to each other to form hard segments[31–33]. The NCO group reacted with the –OH group, carboxylic acid, and amine group on the surface of ACF. Owing to its low surface energy, the perfluoroalkyl group enhanced the hydrophobicity of the surface of the ACF. The different roles of the various chemical structures in the F-PU coating material exhibited a harmonious effect in the resulting ACF membrane.

The FT-IR spectra of the F-PU coating material, TDFO, and IPDI are shown in Fig. 2b. In the FT-IR spectra of the F-PU coating material, the absorption peak at 2270 cm^{-1}, which corresponded to NCO, decreased, and the absorption peak at 3500 cm^{-1}, which corresponded to the OH of TDFO disappeared. Furthermore, two additional peaks were observed at 1705 and 1535 cm^{-1}, which corresponded to the stretching vibration modes of the C=O and N–H bonds in the urethane groups, respectively. In addition, a broad absorption band was observed at ~3340–3320 cm^{-1}, which corresponded to N–H stretching vibration, indicating the generation of –OCOHN– groups in the F-PU coating material. This could be attributed to the fact that PU is capable of forming several kinds of hydrogen bonds owing to the presence of a N–H donor group and a C=O acceptor group in the urethane linkage.

To verify the successful formation of the F-PU in-and-out coating in the coated fabric, the morphology of the bare ACF and

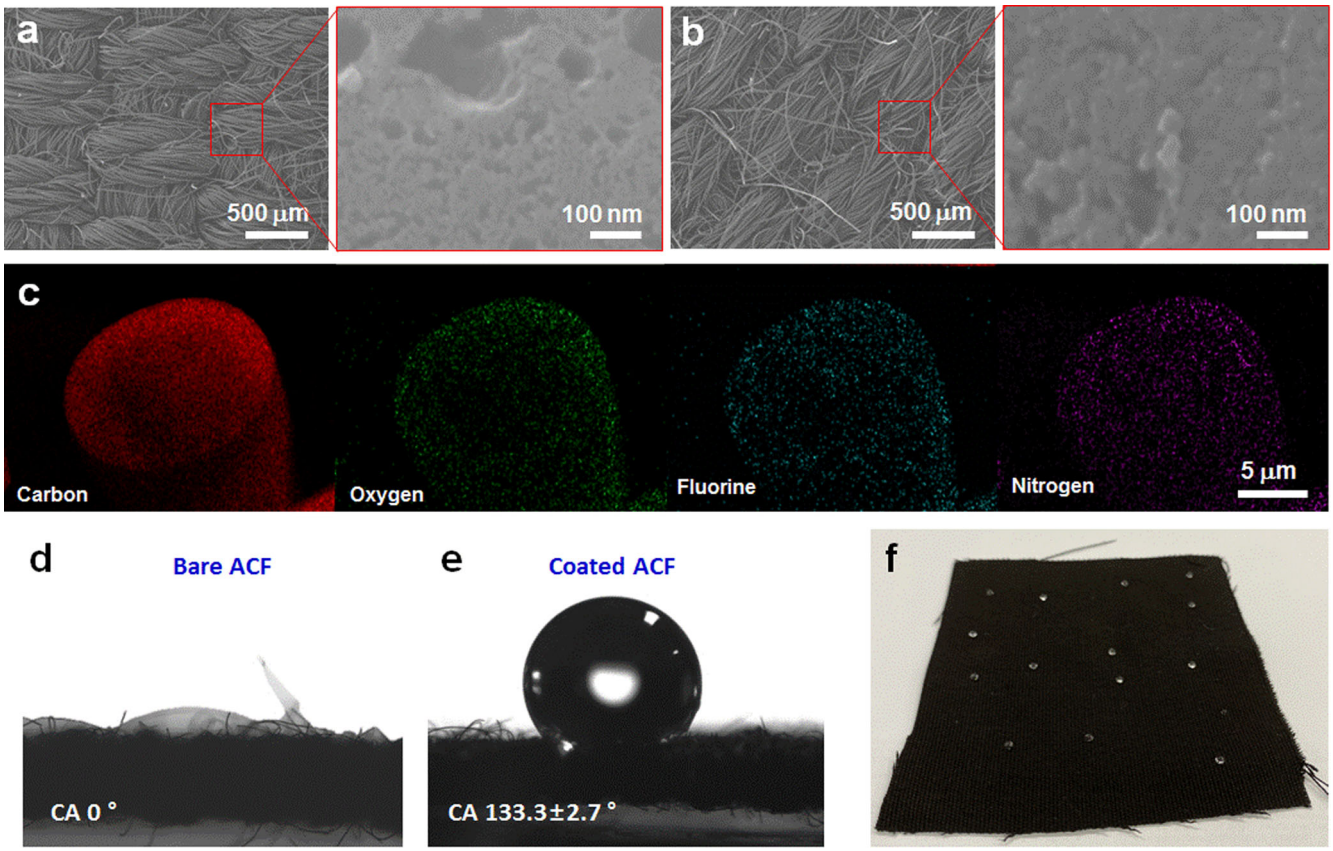

Fig. 3 Characterization of F-PU in-and-out coated ACF. Field emission scanning electron microscopy (FE-SEM) images of (**a**) bare activated carbon fabric (ACF) and (**b**) F-PU in-and-out-coated ACF. **c** FESEM/energy dispersive spectroscopy (EDS) of the F-PU in-and-out-coated ACF (red_carbon, green_oxygen, blue_fluorine, and purple_nitrogen). Contact angle measurement of the (**d**) bare ACF I (**e**) F-PU in-and-out-coated ACF. (**f**) Photographic image of the F-PU in-and-out-coated ACF after immersion in distilled (DI) water (5 uL).

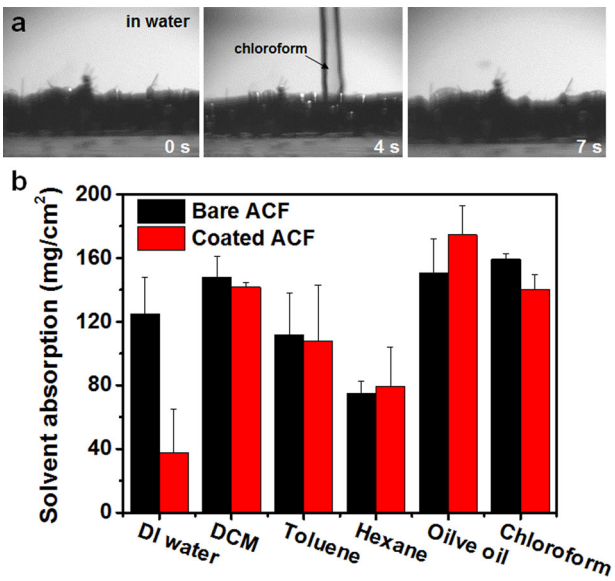

Fig. 4 Wettability and water-oil selective properties of F-PU in-and-out coated ACF. a Photographs of the flow of CF on the F-PU in-and-out-coated ACF in aqueous condition. **b** Absorption capacity (mg/cm2) of the bare ACF and F-PU in-and-out-coated ACF for DI water, dichloromethane (DCM), toluene, hexane, olive oil, and CF. The error bars represent the standard deviations of the data.

F-PU in-and-out-coated ACF were investigated using FESEM/EDS analysis. The FESEM image revealed that the surface of the bare ACF exhibited a high surface roughness and porosity (Fig. 3a). In contrast, after the addition of the F-PU in-and-out coatings, the F-PU in-and-out-coated ACF exhibited a significantly decreased surface roughness and porous structure, which could be attributed to the inflow of F-PU coating materials into the pores of ACF (Fig. 3b). Furthermore, the BET measurements revealed that the specific surface area of the F-PU in-and-out-coated ACF was 11.13 m^2/g, which was 200 times lower than that of the bare ACF. This indicates that the micropore (<2 nm) of the bare ACF was almost completely filled with the in-and-out coating after the F-PU coating treatment (Supplementary Fig. S1).

Although BET has decreased a lot, it is unlikely that flux will decrease because pores <2 nm are lost. The BET analysis results provided information on nano-sized pores, whereas we used porosimeter to confirm the micro-sized space between fibers and fibers according to F-PU coating. There are spaces between fibers within the ACF fabric, and micro-sized spaces rather than nano-sized spaces in this space are very dominant. As shown in the Supplementary Fig. S2, the pore volume can be checked before and after coating. The pore volume slightly decreased after coating, but there were many spaces large enough, so there is no problem with liquid flux.

In addition, these results demonstrate the entry of the F-PU coating materials into the pores of the ACF and their reaction with the functional groups on the surface of ACF. The elemental distribution of the cross–section of the F-PU in-and-out-coated

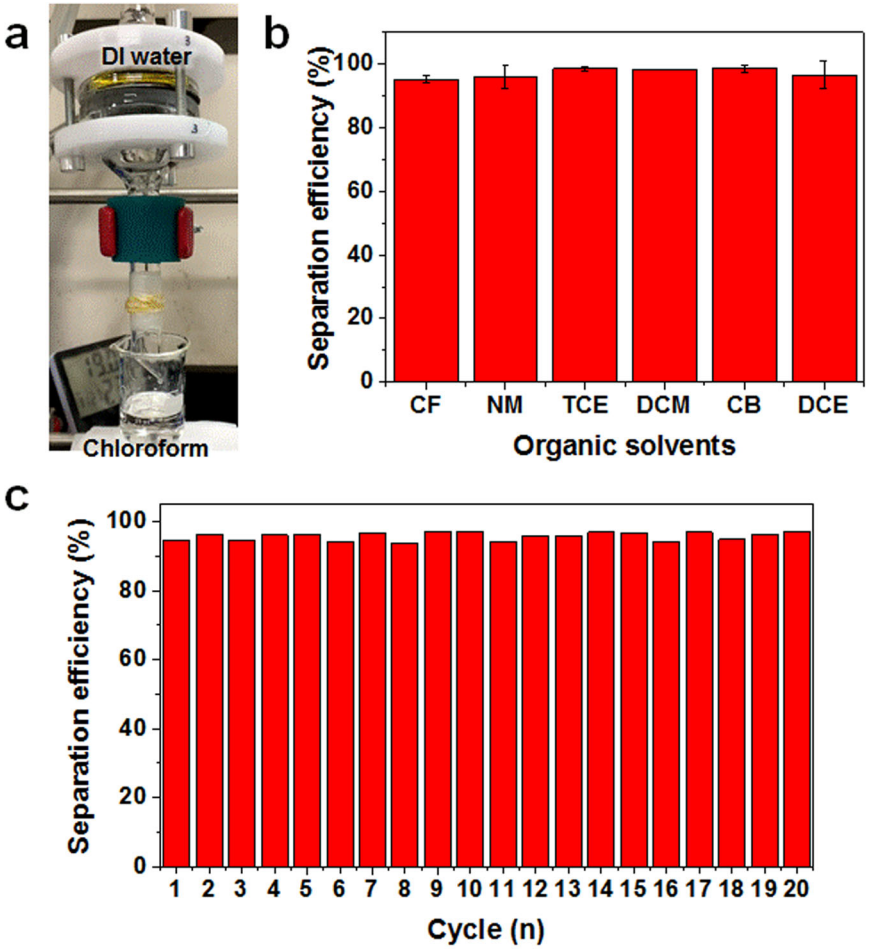

Fig. 5 Oil/water separation performance of F-PU in-and-out coated ACF. a Photograph images of the oil/water separation system containing the F-PU in-and-out coated ACF. **b** Separation efficiencies of the F-PU in-and-out coated ACF for CF/water, nitromethane (NM)/water, Trichloroethylene (TCE)/water, dichloromethane (DCM)/water, chlorobenzene (CB)/water, and 1,2-dichloroethane (DCE)/water mixtures. **c** Separation efficiencies of F-PU in-and-out coated ACF for CF/water mixture as a function of the number of oil/water separation cycles. The error bars represent the standard deviations of the data.

ACF was investigated using FESEM/EDS analysis and XPS (Fig. 3c and Supplementary Fig. S3). The results revealed the presence of fluorine and nitrogen elements from TDFO and urethane bonds inside and outside the F-PU in-and-out-coated ACF. In contrast, only carbon and oxygen elements were observed in the bare ACF (Supplementary Fig. S3). Next, the effect of the TDFO of the F-PU coating materials on the hydrophobicity of the coated ACF was investigated using contact angle analysis. Generally, bare ACF exhibits highly hydrophilic properties because of its polar functional groups. The results revealed that the contact angle of the bare ACF was 0°, and the bare ACF absorbed the water droplet used for the measurement (Fig. 3d). In contrast, the F-PU in-and-out-coated ACF exhibited highly hydrophobic properties with a water contact angle of 133.3 ± 2.7°, and a uniform hydrophobicity (Fig. 3e and f).

The oleophilic and hydrophobic characteristics of the F-PU in-and-out-coated ACF are shown in Fig. 4. In an aqueous condition, oil droplets rapidly spread and were absorbed by the F-PU in-and-out-coated ACF. In contrast, under oil conditions, water droplets were retained on the F-PU in-and-out-coated ACF, and the water contact angle was higher than that under air condition (Supplementary Fig. S4a). In addition, the coated ACF was wetted with oil to form an oil-containing region, which exhibited superhydrophobicity under oil conditions. In contrast, the bare ACF does not selectively absorb oil and water, and exhibited high absorption capacity for all liquid. The F–PU in-and-out-coated ACF exhibited a significantly reduced water absorption capacity; however, its oil absorption capacity was similar to that of the bare ACF (Fig. 4b and Supplementary Fig. S4b). This indicates that the F–PU in-and-out coated ACF exhibited a high selectivity for oil/water mixtures.

Coated fabric has a highly hydrophobic properties and oleophilic properties, whereas bare fabric is hydrophilic and oleophilic. So, once the oil–water solution contacts a surface of the coated fabric, the oil droplets would be quickly adsorbed and spread across the coated fabric because of the synergistic effects of gravity force and high affinity. The interconnected pores between the fibers and the pores within the coated ACF serve as a "high pathway" for oil diffusion. However, the adsorption or diffusion of water would be rejected because of the highly hydrophobic property of perfluorocarbon chain on the coated ACF. Water droplets are inferior due to the competitive adsorption with oil droplets on the surface of coated ACF. Therefore, the water droplets were rejected and the oil droplets spread out as an "oil layer" on the surface of ACF surface.

In addition, because the coated fabric is highly hydrophobic, the breakthrough pressure is a positive value ($\Delta P > 0$) following the equation. So the coated ACF can sustain a certain pressure (negative capillary effect). Without an external pressure, water droplet can't spontaneously penetrate through the coated ACF. On the contrary, when the coated ACF is highly oleophilic ($\theta < 5°$), the breakthrough pressure is a negative value ($\Delta P > 0$), so the

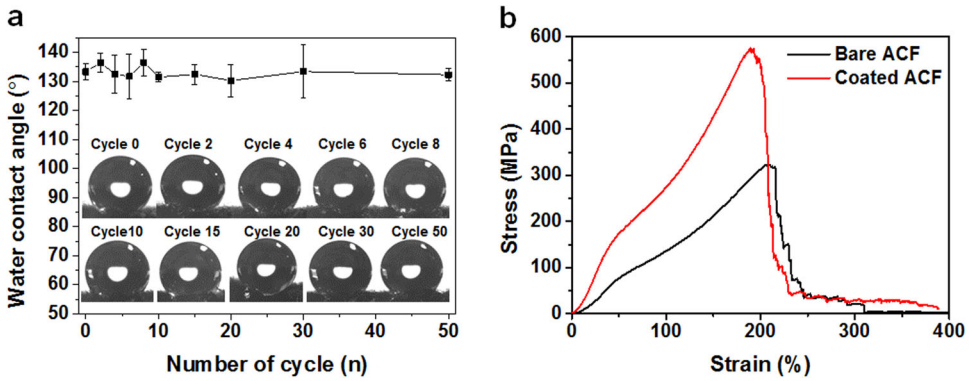

Fig. 6 Durability and mechanical properties of F-PU in-and-out coated ACF. a Water contact angle of the F-PU in-and-out-coated ACF after the scratch test. **b** Tensile strength of the bare ACF and F-PU in-and-out-coated ACF. The error bars represent the standard deviations of the data.

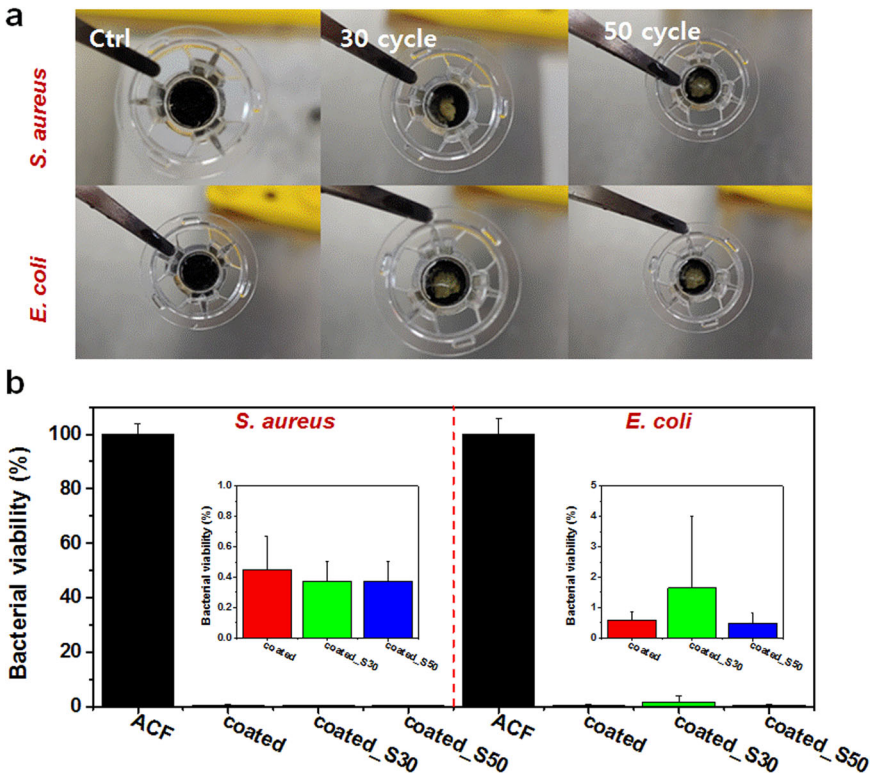

Fig. 7 Bacteria blocking performance of F-PU in-and-out coated ACF. a Photograph images of the bare ACF and the F-PU in-and-out-coated ACF with 30 and 50 scratch cycles after the bacterial penetration tests. **b** Bacterial viability of Staphylococcus aureus (S. aureus) and Escherichia coli (E. coli) for the bare ACF, the F-PU in-and-out coated ACF, and the coated ACF after 30 and 50 scratch cycles (coated_S30 and S50, respectively). The error bars represent the standard deviations of the data.

coated ACF cannot withstand any pressure (capillary effect). The oil droplet are able to permeate the coated ACF spontaneously[34–37].

Based on the aforementioned high hydrophilicity and high oleophilicity of the F-PU in-and-out-coated ACF, The oil–water mixture separation performance of the F-PU in-and-out-coated ACF was examined using a customized oil/water separation system (Fig. 5a). The separation efficiencies of the F-PU in-and-out-coated ACF for various oil–water mixtures were above 95%, indicating the efficient oil–water mixtures separation performance of the F-PU in-and-out-coated ACF for the six mixtures (Fig. 5b). Furthermore, to investigate the reusability of the F-PU in-and-out-coated ACF, the coated ACF was used to separate CF/water mixture for 20 times successively. The material exhibited a remarkable flux rate of above $2 \times 10^4 L \cdot m^{-2} \cdot h^{-1}$ for the CF/water mixture. In addition, the separation efficiency of the material after each application was in the range of 95%, verifying the good stability of the F-PU in-and-out-coated ACF, and its potential for continuous reusability for oil contamination separation (Fig. 5c). These results indicate that the F-PU in-and-out-coated ACFs were ideal reusable separation membranes for the potential treatment of various oily wastewater discharges.

To demonstrate the resistance of the material to external impact and its continuous reusability after impact, the F-PU in-and-out-coated ACF was subjected to a scratch test, and its maintained wettability was investigated. The results revealed that there was a slight change in the water contact angle of the F-PU in-and-out-coated ACF after scratching the coated fabric for 50

times using sand paper (Fig. 6a). In addition, although the scratch test did not induce any significant damage to the F-PU in-and-out coating, the coated ACF membrane maintained its wettability after the occurrence of damages or crack owing to the presence of F-PU in-and-out coatings inside the ACF pores. Moreover, the F-PU in-and-out coating contained numerous urethane chemical structures, which strengthened the intermolecular hydrogen bonds between the hydrogen of the secondary amine group and the carbonyl oxygen. In addition, the F-PU in-and-out coating acted as a physical crosslinker and enhanced the mechanical properties of the ACF. Figure 6b shows a comparison of the stress–strain curve of the bare ACF fabric and the F-PU in-and-out-coated ACF. The tensile strengths of the bare ACF and F-PU in-and-out coated ACF were 322.41 and 575.2 MPa, respectively. The tensile strength of the F-PU in-and-out coated ACF was 1.78 times higher than that of the bare ACF. This indicates that the F-PU in-and-out-coated ACF can withstand further external pressure.

To evaluate the bacterial penetration blocking ability of the F-PU in-and-out-coated ACF, we designed and fabricated a bacterial penetrating system using trans-well plates (Supplementary Fig. S5). To prove that it is not toxic after coating, the C2C12 cell viability test before and after coating was carried out using Cell Counting Kit-8 with a density of 3×104 cells/well for 48 h incubation. Although the viability was slightly reduced in samples with ACF, the cell viability is higher after coating than before coating. This means that there is no toxicity by the coating materials (Supplementary Fig. S6). Anti-bacterial property is the ability of a material to destroy bacteria or suppress their growth or their ability to reproduce. Antibiotics exhibit a very powerful antimicrobial effect; however, they are constantly consumed and exhibit fatal side effects, such as super-bacteria generation. Therefore, separation membranes containing antibiotics are unsuitable in an environment where there is a continuous flow of fluid. This indicates that it is essential to develop separation materials that exhibit anti-fouling properties and high durability.

Figure 7a shows the quantity of bacteria that penetrated through or was retained on the bare ACF and the F-PU in-and-out-coated ACF. No bacteria was observed on the bare ACF owing to its non-selectivity, which enabled the penetration of the *S. aureus* and E. coli. In contrast, numerous light yellow aggregates, which were formed by bacteria colonies, were observed on the surface of the F–PU in-and-out-coated ACF subjected to 30 and 50 scratch cycles. Further experiments were conducted to determine whether the F-PU in-and-out-coated ACF subjected to scratch test can effectively prevent the permeation of bacteria. Bacteria were seeded on the bare ACF and the F–PU in-and-out-coated ACF, cultured for 1 day, after which the OD value of the solution below the inserts of the trans-well plate was measured. The F-PU in-and-out-coated ACF effectively prevented the permeation of *S. aureus* and E. coli by ≥99% (Fig. 7b). Particularly, after the 30- and 50-cycles scratch test, the F-PU in-and-out-coated ACF maintained its bacteria penetration blocking ability for *S. aureus* and E. coli. These results of the performances of the F-PU in-and-out-coated ACF demonstrate the promising potential of the coated -ACF for the prevention of bacterial penetration (≥99%), and its high durability external impact.

In summary, we reported a strategy to modify the surface wettability of porous ACF using F-PU in-and-out coatings. The F-PU coating material was prepared via the reaction of EG, IPDI, and TDFO. The coating of the inner and outer surface of ACF with the F-PU in-and-out coatings was achieved via urethane reactions. The in-and-out coating enabled the formation of a heterogeneous structure in the ACF fabric. The heterogeneous structure of the F-PU in-and-out-coated ACF endowed the fabric with a high durability for scratch resistance. In addition, further investigations revealed that the F-PU in-and-out-coated ACF exhibited goods hydrophobic properties after scratch tests, enhanced tensile strength, oil absorption properties, and excellent oil–water separation performance. Particularly, during the oil–water separation experiments, oils passed through the F-PU in-and-out-coated ACF at a high flux ($2 \times 10^4\ L \cdot m^{-2} \cdot h^{-1}$) and high efficiency (>95%). Lastly, we confirmed that the F-PU in-and-out-coated ACF effectively blocked bacteria permeation regardless of the bacteria type (gram-negative *S. aureus* and gram-positive E. coli), and maintained its bacteria blocking performance after the scratch tests. These results indicate that F-PU in-and-out coating is effective for fabricating a heterogeneous-structured membrane with high durability and excellent bacterial blocking performance.

METHODS

Materials

Activated carbon fabric (ACF, ACC-5092-20) was purchased from Kynol®. The weight, thickness and specific surface area of the ACF were 135 g/m^2, 0.55 mm, and 1800 m^2/g, respectively. Isophorone diisocyanate (IPDI), EG, dimethyl sulfoxide, dichloromethane (DCM), toluene, hexane, olive oil, nitromethane (NM), trichloroethylene (TCE), chlorobenzene (CB), 1,2-dichloroethane (DCE), and chloroform (CF) were purchased from Sigma–Aldrich. 1H,1H,2H,2H-Tridecafluoro-1-n-octanol (TDFO) was obtained from BLD Pharmatech Inc.

Synthesis of F-PU coating materials

First, TDFO–IPDI–EG–IPDI coating materials were synthesized with a two-step addition process, in which the prepolymer was prepared by reacting EG with excess IPDI, after which the end isocyanate (NCO) groups were reacted with the hydroxyl group (–OH) perfluoroalkyl chain of TDFO. The successful preparation of TDFO–IPDI–EG–IPDI coating materials was verified using Fourier transform-infrared (FT–IR) analysis (model 4700 device Jasco, Easton, USA). The molar ratio of IPDI, EG, and TDFO in the prepolymer was 2:1:1. To synthesize the TDFO–IPDI–EG–IPDI coating materials, first, IPDI–EG–IPDI was synthesized by mixing 4.32 mL of IPDI and 0.58 mL of EG in 85.22 mL of DMF, after which the mixture was reacted at 80 °C for 12 h under stirring. Subsequently, 4.66 mL of TDFO was added to the prepared IPDI–EG–IPDI mixture and reacted at 80 °C for 12 h under stirring in an oil bath.

Fabrication of F-PU in-and-out-coated fabric

Generally, ACF contains numerous functional groups including –OH group, ketone, and carboxylic acid. To enhance the reactivity of ACF using the prepared TDFO–IPDI–EG–IPDI coating materials, the ketone of ACF was reduced using sodium borohydride to produce an –OH group. Next, the treated ACF was immersed in TDFO–IPDI–EG–IPDI coating materials solution. Subsequently, the –OH group of ACF and the NCO of TDFO–IPDI–EG–IPDI coating materials were reacted at 80 °C for 72 h in an oil bath.

Characterization of TDFO–IPDI–EG–IPDI in-and-out-coated fabric

The surface morphology and elemental analysis of the TDFO-IPDI-EG-IPDI in-and-out coated fabric were analyzed using X-ray photoelectron spectroscopy (XPS; K-alpha, ThermoFisher Scientific, USA), SEM (IT-500, JEOL, Japan) and field emission scanning electron microscopy equipped with an energy dispersive X-ray spectrometer (FE-SEM/EDS; SUPRA 55VP, Carl Zeiss, Germany). Nitrogen adsorption measurements of TDFO–IPDI–EG–IPDI in-and-out coated fabric were performed using a Brunauer–Emmett–Teller (BET) analyzer (ASAP 2020 system, Micromeritics Instrument Corp., USA). The contact angles of various liquids on the TDFO–IPDI–EG–IPDI in-and-out-coated fabric were evaluated from a contact angle goniometer (Smart Drop Standard, Femtobiomed, Korea). A universal testing

machine (UTM; Model 3366, Instron, USA) was used to measure tensile strength of bare ACF and coated ACF (tensile rate = 5 mm/min^{-1}).

Oil–water absorption and separation

The water or oil absorption of the coated fabric was investigated using six types of test liquids (distilled (DI) water, DCM, toluene, hexane, olive oil, and CF). Feed solution was prepared at a 1:1(v/v) ratio of water and oil. To measure the absorption capacities of the membrane, 1 cm^2 of bare ACF and the in-and-out F-PU-coated ACF was prepared and immersed in the DI water or the oils until the fabrics were totally saturated, after which the samples were removed and immediately weighed. The weight measurement was performed quickly to avoid any absorbate evaporation. The absorption capacity of the bare ACF and in-and-out F-PU-coated ACF was determined in weight:area ratio, as given in Eq. 1:

$$\text{Absorption capacity} = \frac{W_a\,(\text{g}) - W_0(\text{g})}{Area\,(\text{cm}^2)} \quad (1)$$

where W_a is the weight of the bare ACF or in-and-out F-PU-coated ACF in the oil/organic solvents at a saturated state and W_0 is the weight the bare ACF or in-and-out F-PU-coated ACF at the initial state. Each test was repeated three times.

For an oil–water separation test driven only by self-gravity, the bare ACF and in-and-out F-PU-coated ACF were placed between two glass containers. Subsequently, oil–water mixtures were poured onto the bare ACF or in-and-out F-PU coated ACF. Each separation experiment was performed three times, and the separation efficiency was determined using Eq. (2):

$$\text{Separation efficiency} = \frac{V_a}{V_0} \times 100\% \quad (2)$$

Where V_a is the volume of solvent that penetrates to the in-and-out F-PU-coated ACF after the oil–water mixture was poured and V_0 is the volume of solvent in the oil–water mixture before pouring.

The flux (F) of the bare ACF and in-and-out F-PU-coated ACF was calculated using Eq. (3):

$$\text{Flux}\,(F) = \frac{V}{St} \quad (3)$$

where V is the volume of the liquid permeating through the bare ACF and in-and-out F-PU-coated ACF, S is the effective contact area of the bare ACF and in-and-out F-PU-coated ACF, and t is the permeating time.

Bacteria penetration through the F-PU in-and-out-coated fabric

Staphylococcus aureus (*S. aureus*; 25923, ATCC, USA) and *Escherichia coli* (E. coli; 25922, ATCC, USA), which are gram-positive and gram-negative bacteria, respectively, were used in the bacterial penetration blocking experiment. Briefly, both bacteria were cultured in a Tryptic soy broth (soybean–casein digest medium, Becton Dickinson and Company, USA) medium and incubated at 37 °C under aerobic conditions. Subsequently, the bacterial suspension was diluted to an optical density (OD) concentration of 0.1 (measured at 600 nm).

Bare ACF, was used as a control sample, and the coated ACF was used as the experimental sample. All samples used in this experiment were sterilized under ultraviolet-irradiation before culturing with bacterium. The samples were placed in each insert of 24-transwell plates (6.5 mm insert and 8.0 µm diameter pore), after which the inserts were mounted in each well. Subsequently, 0.8 mL of the fresh bacteria culture medium was poured into each well at the bottom of the transwell plate. Thereafter, 80 µL of *S. aureus* or E. coli suspension was added to each insert containing the samples. To validate the experiment, several wells were filled with a pristine medium without bacteria. After incubation of the well plates for 24 h, all inserts were removed from the transwell plates. The OD value of the culture medium remaining at the bottom of each well was measured to evaluate the degree of contamination of the culture medium by bacterial permeation. The OD of the medium was measured at 600 nm using a plate reader.

DATA AVAILABILITY

Data generated and analyzed during this study are included in the present paper. Raw datasets are available from the corresponding author upon request.

Received: 6 January 2022; Accepted: 13 September 2022;
Published online: 23 September 2022

REFERENCES

1. Tanudjaja, H. J., Hejase, C. A., Tarabara, V. V., Fane, A. G. & Chew, J. W. Membrane-based separation for oily wastewater: a practical perspective. *Water Res.* **156**, 347–365 (2019).
2. Joye, S. B. Deepwater Horizon, 5 years on. *Sci.* **349**, 592–593 (2015).
3. Schrope, M. Oil spill: deep wounds. *Nat. N.* **472**, 152–154 (2011).
4. Ivshina, I. B. et al. Oil spill problems and sustainable response strategies through new technologies. *Environ. Sci.: Process Impacts* **17**, 1201–1219 (2015).
5. Kleindienst, S., Paul, J. H. & Joye, S. B. Using dispersants after oil spills: impacts on the composition and activity of microbial communities. *Nat. Rev. Microbiol.* **13**, 388–396 (2015).
6. Li, Y. et al. The forecasting and analysis of oil spill drift trajectory during the Sanchi collision accident, East China Sea. *Ocean Eng.* **187**, 106231 (2019).
7. Yue, X., Li, Z., Zhang, T., Yang, D. & Qiu, F. Design and fabrication of superwetting fiber-based membranes for oil/water separation applications. *Chem. Eng. J.* **364**, 292–309 (2019).
8. Zhang, J. et al. Electrospun flexible nanofibrous membranes for oil/water separation. *J. Mater. Chem. A* **7**, 20075–20102 (2019).
9. Hu, M.-X., Niu, H.-M., Chen, X.-L. & Zhan, H.-B. Natural cellulose microfiltration membranes for oil/water nanoemulsions separation. *Colloids Surf. Physicochem. Eng. Asp.* **564**, 142–151 (2019).
10. Jung, Y. C. & Bhushan, B. Wetting behavior of water and oil droplets in three-phase interfaces for hydrophobicity/philicity and oleophobicity/philicity. *Langmuir* **25**, 14165–14173 (2009).
11. Chen, C., Weng, D., Mahmood, A., Chen, S. & Wang, J. Separation mechanism and construction of surfaces with special wettability for oil/water separation. *ACS Appl. Mater. Interfac.* **11**, 11006–11027 (2019).
12. Liu, Y. et al. On-demand oil/water separation of 3D Fe foam by controllable wettability. *Chem. Eng. J.* **331**, 278–289 (2018).
13. Tian, X., Jokinen, V., Li, J., Sainio, J. & Ras, R. H. Unusual dual superlyophobic surfaces in oil–water systems: the design principles. *Adv. Mater.* **28**, 10652–10658 (2016).
14. Lin, X. et al. Cobweb-inspired superhydrophobic multiscaled gating membrane with embedded network structure for robust water-in-oil emulsion separation. *ACS Sustain. Chem. Eng.* **5**, 3448–3455 (2017).
15. Lin, X., Heo, J., Choi, M. & Hong, J. Simply realizing durable dual Janus superwettable membranes integrating underwater low-oil-adhesive with super-water-repellent surfaces for controlled oil–water permeation. *J. Membr. Sci.* **580**, 248–255 (2019).
16. Lin, X., Park, S., Choi, D., Heo, J. & Hong, J. Mechanically durable superhydrophobic PDMS-candle soot composite coatings with high biocompatibility. *J. Ind. Eng. Chem.* **74**, 79–85 (2019).
17. Heo, J. et al. Highly permeable graphene oxide/polyelectrolytes hybrid thin films for enhanced CO 2/N 2 separation performance. *Sci. Rep.* **7**, 1–8 (2017).
18. Hong, J. & Kang, S. W. Hydrophobic properties of colloidal films coated with multi-wall carbon nanotubes/reduced graphene oxide multilayers. *Coll. Surf. Physicochem. Eng. Asp.* **374**, 54–57 (2011).
19. Heo, J., Choi, M. & Hong, J. Facile surface modification of polyethylene film via spray-assisted layer-by-layer self-assembly of graphene oxide for oxygen barrier properties. *Sci. Rep.* **9**, 1–7 (2019).
20. Patel, M., Patel, J., Pawar, Y., Patel, N. & Shah, M. Membrane-based downhole oil–water separation (DOWS) technology: an alternative to hydrocyclone-based DOWS. *J. Pet. Explor. Prod. Technol.* **10**, 2079–2088 (2020).
21. Amran, N. A. & Mustapha, S. N. A. In *Resources of Water* (IntechOpen, 2020).

22. Adetunji, A. I. & Olaniran, A. O. Treatment of industrial oily wastewater by advanced technologies: a review. *Appl. Water Sci.* **11**, 1–19 (2021).
23. Yu, L., Han, M. & He, F. A review of treating oily wastewater. *Arab. J. Chem.* **10**, S1913–S1922 (2017).
24. Wang, Y. et al. Beads-on-string structured nanofibers for smart and reversible oil/water separation with outstanding antifouling property. *ACS Appl. Mater. Interfac.* **8**, 25612–25620 (2016).
25. Xu, H., Liu, H., Huang, Y. & Xiao, C. Three-dimensional structure design of tubular polyvinyl chloride hybrid nanofiber membranes for water-in-oil emulsion separation. *J. Membr. Sci.* **620**, 118905 (2021).
26. Qing, W. et al. In situ silica growth for superhydrophilic-underwater superoleophobic Silica/PVA nanofibrous membrane for gravity-driven oil-in-water emulsion separation. *J. Membr. Sci.* **612**, 118476 (2020).
27. Choi, D. et al. Nano-film coatings onto collagen hydrogels with desired drug release. *J. Ind. Eng. Chem.* **36**, 326–333 (2016).
28. Park, K., Choi, D. & Hong, J. Nanostructured polymer thin films fabricated with brush-based layer-by-layer self-assembly for site-selective construction and drug release. *Sci. Rep.* **8**, 1–9 (2018).
29. Roose-Amsaleg, C. & Laverman, A. M. Do antibiotics have environmental side-effects? Impact of synthetic antibiotics on biogeochemical processes. *Environ. Sci. Pollut. Res.* **23**, 4000–4012 (2016).
30. Ning, L., De-Ning, W. & Sheng-Kang, Y. Hydrogen-bonding properties of segmented polyether poly (urethane urea) copolymer. *Macromolecules* **30**, 4405–4409 (1997).
31. Chavan, J. G., Rath, S. K., Praveen, S., Kalletla, S. & Patri, M. Hydrogen bonding and thermomechanical properties of model polydimethylsiloxane based poly (urethane-urea) copolymers: effect of hard segment content. *Prog. Org. Coat.* **90**, 350–358 (2016).
32. Ning, L., De-Ning, W. & Sheng-Kang, Y. Crystallinity and hydrogen bonding of hard segments in segmented poly (urethane urea) copolymers. *Polymer* **37**, 3577–3583 (1996).
33. Cao, G., Wang, Y., Wang, C. & Ho, S.-H. A dually prewetted membrane for continuous filtration of water-in-light oil, oil-in-water, and water-in-heavy oil multiphase emulsion mixtures. *J. Mater. Chem. A* **7**, 11305–11313 (2019).
34. Cao, H., Gu, W., Fu, J., Liu, Y. & Chen, S. Preparation of superhydrophobic/oleophilic copper mesh for oil-water separation. *Appl. Surf. Sci.* **412**, 599–605 (2017).
35. Yong, J., Huo, J., Chen, F., Yang, Q. & Hou, X. Oil/water separation based on natural materials with super-wettability: recent advances. *PCCP* **20**, 25140–25163 (2018).
36. Ma, W., Zhang, M., Liu, Z., Huang, C. & Fu, G. Nature-inspired creation of a robust free-standing electrospun nanofibrous membrane for efficient oil–water separation. *Environ. Sci. Nano* **5**, 2909–2920 (2018).
37. Li, K. et al. Facile fabrication of superhydrophilic/underwater superoleophobic polyvinyl acetate/sodium silicate composite coating for the effective water/oil separation and the study on the anti-fouling property, durability and separation mechanism. *Prog. Org. Coat.* **150**, 105979 (2021).

ACKNOWLEDGEMENTS

This work was supported by Korea Environment Industry & Technology Institute (KEITI) through the Ecological Imitation-based Environmental Pollution Management Technology Development Project, funded by Korea Ministry of Environment (MOE) (2019002790001). This work was supported by the National Research Foundation of Korea (NRF) grant funded by the Korea government (MSIT)(No. 2021R1A4A3030268). This work was supported by the Agency for Defense Development under project 912762101.

AUTHOR CONTRIBUTIONS

All authors have contributed to writing this paper and have given approval to the final version of the paper. In detail, M.C. conceptualized and planned the experiments. S.P. designed and did bacteria experiments. W.C performed the stress-strain experiments. Y.K. and K.M.C. prepared the coating materials and ACF. J.H., M.K.K., and H.J. contributed to paper writing and editing. Y.J. and S.L. supervised the project. J.H. supervised and prepared the paper.

COMPETING INTERESTS

The authors declare no competing interests.

ADDITIONAL INFORMATION

Supplementary information The online version contains supplementary material available at https://doi.org/10.1038/s41545-022-00191-0.

Correspondence and requests for materials should be addressed to Youngho Jin, Sangmin Lee or Jinkee Hong.

Reprints and permission information is available at http://www.nature.com/reprints

Publisher's note Springer Nature remains neutral with regard to jurisdictional claims in published maps and institutional affiliations.